Scale-Reconstructable Structure from Motion Using Refraction with a Single Camera

Akira Shibata[1], Hiromitsu Fujii[1], Atsushi Yamashita[1], and Hajime Asama[1]

Abstract — Three-dimensional (3D) measurement is an important means for robots to acquire information about their environment. Structure from Motion is one of these 3D measurement methods. The 3D reconstruction of objects in the environment can be obtained from pictures captured with single camera in Structure from Motion. Furthermore, the camera motion can be obtained simultaneously. Because of its simplicity, Structure from Motion has been implemented in various ways. However there is an essential problem in that the scale of the measured objects cannot be computed by Structure from Motion. In order to compute the absolute scale, other information is required. However this is difficult for robots in an unknown situation. In this paper, we propose a method that can reconstruct the absolute scale of objects using refraction. Refraction changes the light ray path between the objects and the camera. This method is implemented using only a refractive plate and single camera. The results of simulations show the effectiveness of the proposed method in both air and other media (e.g., water).

I. INTRODUCTION

A remote control robot is an important technology that is needed to explore areas too dangerous for people, such as nuclear plants or disaster sites. These robots need detailed information about their surrounding situation to conduct their activities. In order to acquire the position of surrounding objects, 3D measurement methods are required.

Structure from Motion is a 3D measurement method that is extensively studied in computer vision [1]. With this method, we can simultaneously estimate both the 3D structure of objects and the motion of the camera (rotational and translational parameters) with a single camera. Because of the flexibility of camera motion, Structure from Motion is suited to robot sensing. However, it is impossible to determine absolute translational parameters from the images alone. This is because when the scale of both scene and camera transfer change according to the same ratio, the camera will capture the same images that cannot be distinguished from the earlier ones. As a result, the absolute 3D structure of the objects in the scene cannot be estimated. In order to obtain absolute scale with Structure from Motion using a single camera, other information such as absolute scale in the scene or constraints on the camera motion is required [1]–[4]. However, it is difficult to add scale information when exploring an unknown environment by remote control robot. Furthermore constraints on the camera motion decrease the flexibility of Structure from Motion. Therefore, another approach to reconstruct the scale is required.

[1] A. Shibata, H. Fujii, A. Yamashita and H. Asama are with Department of Precision Engineering, The University of Tokyo, 7-3-1 Hongo, Bunkyo-ku, Tokyo 113-8656, Japan shibata@robot.t.u-tokyo.ac.jp
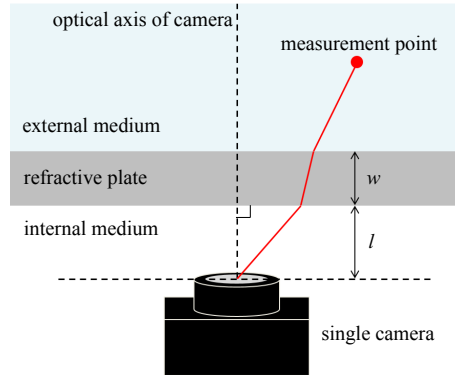
Fig. 1. System of the proposed method. The refractive plate is located between the camera and scene objects.

In this paper, we propose an absolute Structure from Motion method using refraction. Refraction changes the light ray path, which causes images to differ, even if the scale of both scene and camera transfer change at the same ratio. This difference enables us to compute the absolute translational parameter and reconstruct 3D objects. The proposed method is implemented with a simple system composed of a refractive plate and a single camera.

II. RELATED WORK

Refraction occurs when a light ray passes though the boundary surface between different media (e.g., air and water). It is well known that the direction of the light ray changes in accordance with Snell's law [5]–[13]. Refractive geometry in computer vision is a well studied topic, especially for underwater environments [5]–[8]. However these studies focused on removing the effect of refraction as distortion. On the other hand, the proposed method uses refraction actively to reconstruct the scale of objects.

Refraction is used for 3D measurement in several studies. The depth map is obtained from the difference of two images with and without the refractive plate between the camera and the scene [9]. In another study, the depth map was obtained from images captured through a refractive plate rotating around the optical axis of the camera [10]. Furthermore, there are studies on 3D measurement from single images with refractive objects such as a biprism [11] or special waterproof case [12]. These studies measure 3D scenes using active refraction. However, the measurement range is limited. Therefore, these methods are not suited to the large-scale measurement that is required by an exploring robot. In contrast, the proposed method can measure a wider range than the other methods using refraction.
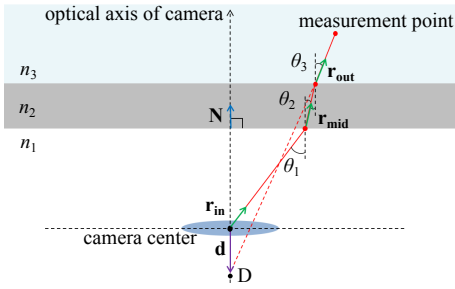
Fig. 2. Light ray passing through a refractive plane. Refraction occurs twice between the camera and objects according to Snell's law. There are three vectors: $\mathbf{r}_{in}$, $\mathbf{r}_{mid}$ and $\mathbf{r}_{out}$.
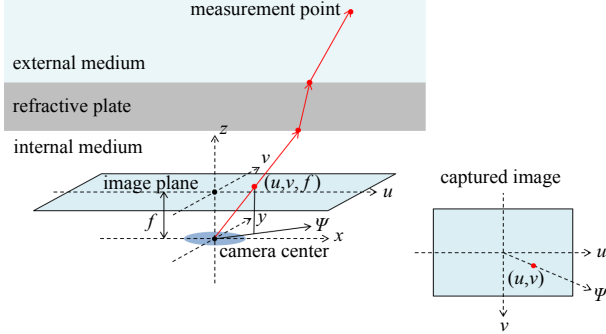
Fig. 3. Vector $\mathbf{r}_{in}$ is obtained from the image coordinates. Because the refractive vectors are on the same plane, we can obtain $\mathbf{r}_{mid}$ and $\mathbf{r}_{out}$ using Snell's law.

III. MESUREMENT METHOD

A. Refractive Plate System

The system of this method is shown in Fig. 1. We use a general single camera that is calibrated and place a refractive plate between the camera and the scene objects. The refractive plate should be placed such that its surface is orthogonal to the optical axis of the camera. The distance between the camera and refractive plate l as well as the thickness of the refractive plate w are known. Let the medium between the camera and refractive plate be the internal medium, and the medium between refractive plate and the measurement object be the external medium. The refractive indices of these media are known.

B. Light Ray Path Tracing

In this section, the path the light traces from image points to 3D points considering refraction is explained. The light ray refracts at both faces of the refractive plate. Therefore, three different ray vectors exist between the camera center and the object. Let the unit vectors of the ray from the camera to the measurement object be $\mathbf{r}_{in} = (\alpha_1, \beta_1, \gamma_1)^T$, $\mathbf{r}_{mid} = (\alpha_2, \beta_2, \gamma_2)^T$ and $\mathbf{r}_{out} = (\alpha_3, \beta_3, \gamma_3)^T$, respectively. These vectors and the normal vector of the refractive plate are on the same plane (Fig. 2). On this plane, θ_1 and θ_2 are the angle of the incident light and refractive light from the internal medium to the refractive plate, respectively. In addition, θ_3 is the angle of refractive light from the refractive plate to the external medium. The relation between these angles are

explained by Snell's law as follows.

$$n_1 \sin\theta_1 = n_2 \sin\theta_2, \tag{1}$$
$$n_2 \sin\theta_2 = n_3 \sin\theta_3, \tag{2}$$

where n_1, n_2 and n_3 are the refractive indices of the internal medium, refractive plate and external medium, respectively.

Using these relations, $\mathbf{r}_{in}$, $\mathbf{r}_{mid}$ and $\mathbf{r}_{out}$ can be computed. First, $\mathbf{r}_{in}$ can be computed from the coordinates of the image point. When the coordinates of the image point are (u, v) and the focal length of camera is f, $\mathbf{r}_{in}$ is expressed as normalized (u, v, f) (Fig. 3). Furthermore, we define the ψ-axis whose direction is a projection of $\mathbf{r}_{in}$ on the x-y plane. The refraction occurs on the ψ-z plane.

Next, $\mathbf{r}_{mid}$ can be computed. Because the three vectors $\mathbf{r}_{in}$, $\mathbf{r}_{mid}$ and the normal vector of the refractive plate $\mathbf{N} = (0, 0, 1)$ are on the same plane, $\mathbf{r}_{mid}$ is expressed as follows.

$$\mathbf{r}_{mid} = \begin{pmatrix} \alpha_2 \\ \beta_2 \\ \gamma_2 \end{pmatrix} = p_1 \begin{pmatrix} \alpha_1 \\ \beta_1 \\ \gamma_1 \end{pmatrix} + q_1 \begin{pmatrix} 0 \\ 0 \\ 1 \end{pmatrix}, \tag{3}$$

where p_1 and q_1 are constant.

Next, $\cos\theta_1$ is calculated from the inner product of $\mathbf{r}_{in}$ and $\mathbf{N}$.

$$\mathbf{r}_{in} \cdot \mathbf{N} = |\mathbf{r}_{in}||\mathbf{N}|\cos\theta_1, \tag{4}$$
$$\therefore \cos\theta_1 = \gamma_1, \tag{5}$$

and $\sin\theta_1$ is calculated from the cross product of $\mathbf{r}_{in}$ and $\mathbf{N}$.

$$|\mathbf{r}_{in} \times \mathbf{N}| = |\mathbf{r}_{in}||\mathbf{N}|\sin\theta_1, \tag{6}$$
$$\therefore \sin\theta_1 = \sqrt{(\alpha_1)^2 + (\beta_1)^2}. \tag{7}$$

Furthermore, $\cos\theta_2$ is calculated from the inner product of $\mathbf{r}_{mid}$ and $\mathbf{N}$.

$$\mathbf{r}_{mid} \cdot \mathbf{N} = |\mathbf{r}_{mid}||\mathbf{N}|\cos\theta_2, \tag{8}$$
$$\therefore \cos\theta_2 = \gamma_2 = p_1\gamma_1 + q_1, \tag{9}$$

and $\sin\theta_2$ is calculated from the cross product of $\mathbf{r}_{mid}$ and $\mathbf{N}$.

$$|\mathbf{r}_{mid} \times \mathbf{N}| = |\mathbf{r}_{mid}||\mathbf{N}|\sin\theta_2, \tag{10}$$
$$\therefore \sin\theta_2 = \sqrt{(\alpha_2)^2 + (\beta_2)^2}$$
$$= \sqrt{(p_1\alpha_1)^2 + (p_1\beta_1)^2}. \tag{11}$$

From Eqs. (1), (7) and (11), p_1 is obtained.

$$p_1 = \frac{\sin\theta_2}{\sin\theta_1} = \frac{n_1}{n_2}. \tag{12}$$

From Eqs. (5), (9) and (12), $\cos\theta_2$ is expressed.

$$\cos\theta_2 = p_1\gamma_1 + q_1 = \frac{n_1}{n_2}\cos\theta_1 + q_1. \tag{13}$$

We note that $\cos\theta_2$ can also be expressed as follows according to its trigonometric identity,

$$\cos\theta_2 = \sqrt{1 - \sin^2\theta_2} = \sqrt{1 - \left(\frac{n_1}{n_2}\right)^2 \sin^2\theta_1}. \tag{14}$$

From Eqs. (13) and (14), q_1 is obtained.

$$q_1 = -\frac{n_1}{n_2}\cos\theta_1 + \sqrt{1 - \left(\frac{n_1}{n_2}\right)^2 \sin^2\theta_1}. \quad (15)$$

Therefore, from Eqs. (3), (12) and (15), we can calculate $\mathbf{r}_{\mathrm{mid}}$.

$$\mathbf{r}_{\mathrm{mid}} = \frac{n_1}{n_2}\mathbf{r}_{\mathrm{in}}$$
$$- \left\{\frac{n_1}{n_2}\cos\theta_1 - \sqrt{1 - \left(\frac{n_1}{n_2}\right)^2 \sin^2\theta_1}\right\}\mathbf{N}. \quad (16)$$

Vector $\mathbf{r}_{\mathrm{out}}$ is computed by the same procedure.

$$\mathbf{r}_{\mathrm{out}} = \frac{n_2}{n_3}\mathbf{r}_{\mathrm{mid}}$$
$$- \left\{\frac{n_2}{n_3}\cos\theta_2 - \sqrt{1 - \left(\frac{n_2}{n_3}\right)^2 \sin^2\theta_2}\right\}\mathbf{N}. \quad (17)$$

Here, let the intersection point of $\mathbf{r}_{\mathrm{out}}$ and the optical axis of camera be start point D, whose position vector is expressed as follows.

$$\mathbf{d} = (0, 0, d), \quad (18)$$

where d is distance between point D and the camera center, which is calculated geometrically (Fig. 2).

$$d = l + w - \frac{l\tan\theta_1 + w\tan\theta_2}{\tan\theta_3}. \quad (19)$$

C. Geometrical Relation

An object to be measured is observed from two different viewpoints in Structure from Motion. These two camera coordinates are C and C' respectively. The z-axis of each coordinate corresponds to each optical axis of the camera and the world coordinates correspond to the camera coordinates C. The rotation matrix $\mathbf{R}$ is a transformation matrix from camera coordinate C to C', and transfer vector $\mathbf{t}$ is defined as the position vector of the center of the camera coordinate C'. Vector $\mathbf{r}_{\mathrm{out}}$ and $\mathbf{d}$ of each coordinate point can be expressed as follows.

$$\mathbf{r}_{\mathrm{out}} = (x, y, z)^{\mathrm{T}}, \quad (20)$$
$$\mathbf{d} = (0, 0, d)^{\mathrm{T}}, \quad (21)$$
$$\mathbf{r}'_{\mathrm{out}} = (x', y', z')^{\mathrm{T}}, \quad (22)$$
$$\mathbf{d}' = (0, 0, d')^{\mathrm{T}}. \quad (23)$$

Each of the $\mathbf{r}_{\mathrm{out}}$ vectors of the two coordinates and the vector between each of the start points D of both coordinates are on the same plane (Fig. 4). These three vectors are expressed in world coordinates as $\mathbf{r}_{\mathrm{out}}$, $\mathbf{R}^{-1}\mathbf{r}'_{\mathrm{out}}$ and $\mathbf{t} + \mathbf{R}^{-1}\mathbf{d}' - \mathbf{d}$. Therefore, we obtain the equation for this geometrical relation as follows.

$$\left\{(\mathbf{t} + \mathbf{R}^{-1}\mathbf{d}' - \mathbf{d}) \times \mathbf{R}^{-1}\mathbf{r}'_{\mathrm{out}}\right\}^{\mathrm{T}}\mathbf{r}_{\mathrm{out}} = 0. \quad (24)$$

If there is no refractive plate, Eq. (24) holds when vector $\mathbf{t}$ is multiplied. This is the reason why the scale of vector $\mathbf{t}$ can not be acquired by conventional method.
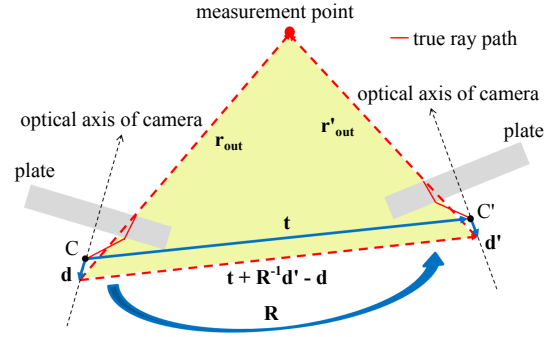
Fig. 4. In the refraction scenario, the geometrical relation changes such that the two vectors ($\mathbf{r}_{\mathrm{out}}$ and $\mathbf{r}'_{\mathrm{out}}$) and the vector between the start points of each camera position are on the same plane.

Equation (24) can be converted into a formula consisting of an inner product of the vector $\mathbf{u}$, composed of known quantities and vector $\mathbf{g}$, composed of unknown quantities by the orthonormality of rotation matrix.

$$\begin{pmatrix} xx' \\ yx' \\ zx' \\ xy' \\ yy' \\ zy' \\ xz' \\ yz' \\ zz' \\ dyx' + d'xy' \\ -dxx' + d'yy' \\ d'zy' \\ dyy' - d'xx' \\ -dxy' - d'yx' \\ -d'zx' \\ dyz' \\ -dxz' \end{pmatrix}^{\mathrm{T}} \begin{pmatrix} r_{12}t_3 - r_{13}t_2 \\ r_{13}t_1 - r_{11}t_3 \\ r_{11}t_2 - r_{12}t_1 \\ r_{22}t_3 - r_{23}t_2 \\ r_{23}t_1 - r_{21}t_3 \\ r_{21}t_2 - r_{22}t_1 \\ r_{32}t_3 - r_{33}t_2 \\ r_{33}t_1 - r_{31}t_3 \\ r_{31}t_2 - r_{32}t_1 \\ r_{11} \\ r_{12} \\ r_{13} \\ r_{21} \\ r_{22} \\ r_{23} \\ r_{31} \\ r_{32} \end{pmatrix} = 0, \quad (25)$$

$$\iff \mathbf{u}^{\mathrm{T}}\mathbf{g} = 0, \quad (26)$$

where r_{ij} is the i, j-th element of rotational matrix $\mathbf{R}$, and t_{i} is the i-th element of transfer vector $\mathbf{t}$.

Because Eq. (26) is obtained from every measurement point, a homogeneous equation is obtained from n points.

$$\mathbf{Ug} = \mathbf{0}, \quad (27)$$

where

$$\mathbf{U} = (\mathbf{u}_1, \mathbf{u}_2, \mathbf{u}_3, \cdots, \mathbf{u}_n)^{\mathrm{T}}. \quad (28)$$

In order to compute the unknown vector $\mathbf{g}$, a least-squares method is applied to Eq. (27). Let g_{i} be the i-th element of $\mathbf{g}$. Then $g_{10} \sim g_{12}$ and $g_{13} \sim g_{15}$ are the same as the first and second columns of $\mathbf{R}$ respectively. This leads to two constraints because of the orthonormality of the rotation matrix.

$$g_{10}^2 + g_{11}^2 + g_{12}^2 = 1, \quad (29)$$
$$g_{13}^2 + g_{14}^2 + g_{15}^2 = 1. \quad (30)$$

The norm of **g** is determined uniquely because of Eqs. (29) and (30), which enable us to estimate the absolute scale of the transfer vector and scene objects. These constraints are applied to the least-squares method using the Lagrange multiplier method.

D. Computing the Rotation Matrix and Transfer Vector

Rotation matrix **R** and transfer vector **t** are computed from elements of **g**. The first and second columns of **R** are the same as $g_{10} \sim g_{15}$, and the third column of **R** can be calculated using orthonormality.

$$
\begin{pmatrix} g_{10} \\ g_{11} \\ g_{12} \end{pmatrix} \times \begin{pmatrix} g_{13} \\ g_{14} \\ g_{15} \end{pmatrix} = \begin{pmatrix} r_{10} \\ r_{11} \\ r_{12} \end{pmatrix} \times \begin{pmatrix} r_{13} \\ r_{14} \\ r_{15} \end{pmatrix}
$$

$$
= \begin{pmatrix} r_{31} \\ r_{32} \\ r_{33} \end{pmatrix}. \tag{31}
$$

The transfer vector is computed using the decomposition of matrix **E** that includes $g_1 \sim g_9$.

$$
\begin{aligned}
\mathbf{E} &= \begin{pmatrix} g_1 & g_2 & g_3 \\ g_4 & g_5 & g_6 \\ g_7 & g_8 & g_9 \end{pmatrix} \\
&= \begin{pmatrix} r_{12}t_3 - r_{13}t_2 & r_{13}t_1 - r_{11}t_3 & r_{11}t_2 - r_{12}t_1 \\ r_{22}t_3 - r_{23}t_2 & r_{23}t_1 - r_{21}t_3 & r_{21}t_2 - r_{22}t_1 \\ r_{32}t_3 - r_{33}t_2 & r_{33}t_1 - r_{31}t_3 & r_{31}t_2 - r_{32}t_1 \end{pmatrix} \\
&= \mathbf{RT}, \tag{32}
\end{aligned}
$$

$$
\therefore \mathbf{T} = \mathbf{R}^{-1}\mathbf{E}, \tag{33}
$$

where

$$
\mathbf{T} = \begin{pmatrix} 0 & -t_3 & t_2 \\ t_3 & 0 & -t_1 \\ -t_2 & t_1 & 0 \end{pmatrix}. \tag{34}
$$

Therefore, the transfer vector can be obtained from elements of **T**.

After the camera motion is computed, the 3D coordinates of the points to be measured are computed by triangulation. The intersection point of the $\mathbf{r}_{\mathrm{out}}$ vectors of both calculated camera positions forms the estimated point position. If the $\mathbf{r}_{\mathrm{out}}$ vectors do not intersect because of the error, the center of the orthogonal line of both vectors is the estimated position which should be the nearest point to both vectors.

E. Application to Measurement in Air

The proposed method is general because internal and external media are not specified. It can be applied as long as the refractive indices of those media are known. For example, this method can be used for underwater measurement. However, in this section, we focus on measurement in air because many 3D measurements occur in air in practice. The refractive index of air is approximately 1.00. When both external and internal media are air, $n_1 = n_3 = 1.00$ and $\theta_1 = \theta_3$ modified from Eqs. (1) and (2), respectively, hold. Therefore, Eq. (19) is modified as follows.

$$
d = w - \frac{w \tan\theta_2}{\tan\theta_1}. \tag{35}
$$

TABLE I
SIMULATION CONDITIONS

Situation	Air
n_1	1.0 (air)
n_2	1.49 (acryl)
n_3	1.0 (air)
l	200 [mm]
w	50 [mm]
R	(-0.15π,-0.15π, 0.1π) [rad] (Euler angles)
t	(600, -300, 50) [mm]
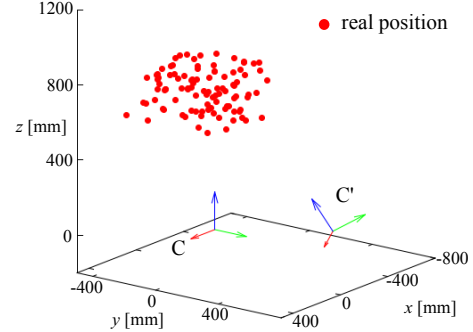
Fig. 5. In the simulation, camera positions are given. Blue vectors indicates the optical axis of each camera. One hundred points (red circles) are placed randomly in 3D space such that each camera can capture all of them.
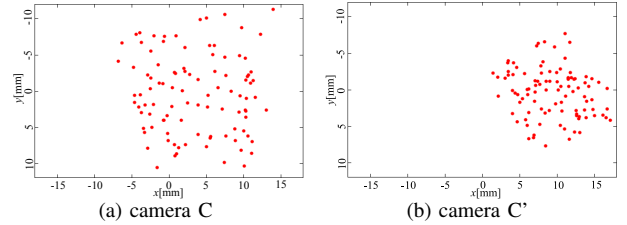
(a) camera C   (b) camera C'

Fig. 6. Images captured by both cameras in the simulation.

In Eq. (35), distance d has no relation to the length l between the refractive plate and camera center. Because both internal and external media are air, $\mathbf{r}_{\mathrm{in}}$ and $\mathbf{r}_{\mathrm{out}}$ are parallel. Therefore, the distance between these vectors does not change with respect to l. Other calculation procedures are the same as the above method.

IV. SIMULATION EXPERIMENTS

A. Simulation in Air

In order to validate the effectiveness of the proposed method, a simulation experiment was conducted. Simulation conditions are shown in Table I. We placed 100 measurement points randomly in a 3D space where both cameras could capture all of them. The blue vectors indicate the optical axis of each camera in Fig. 5. First, images of all the points for both cameras as captured through the refractive plates were simulated (Fig. 6). From those image coordinates, the 3D coordinates of the points were computed using the proposed method and compared with the true position of the points.
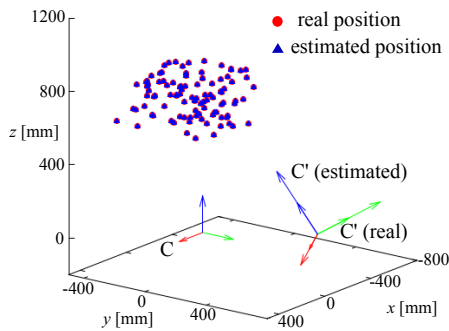
Fig. 7. Simulation results of the proposed method (in air). The distances between the real position (red dots) and estimated position (blue triangles) are extremely small. This shows that the proposed method can reconstruct scene objects with absolute scale
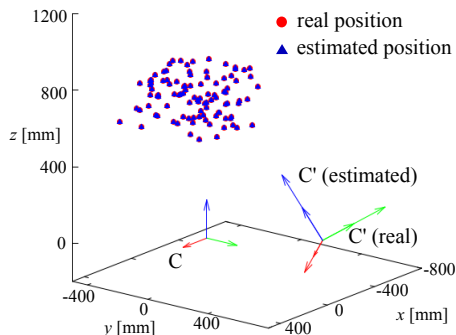
Fig. 8. Simulation results of the proposed method (in water). This shows that the proposed method is effective in water.

The result is shown in Fig. 7. The red circles indicate the real positions and the blue triangles indicate their estimated positions. It is clear that the points were reconstructed correctly. The average of each Euclidean distance between the true and reconstructed positions was extremely small (8.6×10^{-6}mm). Therefore, the proposed method can reconstruct the scale of a scene object.

B. Simulation in Water

In order to ensure the effectiveness of proposed method in a general situation, a simulation experiment in water was also conducted. The conditions were the same as those of the air simulation (Table I), excluding n_3. The refractive index of water was set to $n_3 = 1.33$ in this simulation. The result is shown in Fig. 8. The average of each Euclidean distance between the true and reconstructed positions was extremely small (1.1×10^{-7}mm). Therefore, the proposed method can reconstruct the scale of scene objects in water as well as in air. This indicates that if the internal and external media are different, the proposed method is still effective.

C. Influence of Refractive Plate Thickness

The proposed method makes use of refraction to reconstruct the absolute scale of the objects. Therefore, it is assumed that the precision of the reconstruction would be improved by increasing the effect of refraction. In this system, the refraction is generated by the refractive plate, and its effect changes according to the thickness of the plate.
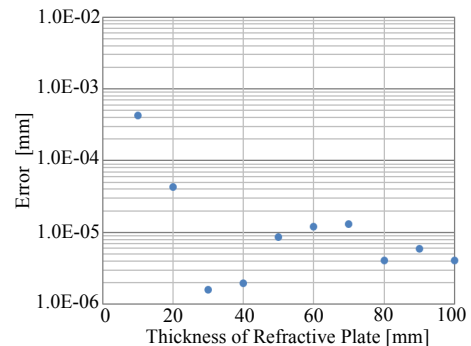
Fig. 9. Error for various thicknesses of refractive plate. The horizontal axis is the thickness of the plate w, and the vertical axis is the distance between the true positions and estimated positions. This indicates that the precision of measurement is improved when the plate is thicker.

In this section, the thickness of the plate was changed in the simulation to investigate the influence of thickness.

The thickness of refractive plate w was changed by 10 mm (from 10 to 100 mm), and the error of the reconstruction results were compared. In this experiment, the distance between the camera center and refractive plate l as well as the positions of the data points were the same as for previous experiments (Table I). The medium of this simulation was air. The result is shown in Fig. 9. The horizontal axis is the thickness of the plate w, and the vertical axis is the amount of error between the true and estimated positions. This indicates that the precision of the measurement is improved when the plate is thicker. Therefore, in the proposed method, the grater the amount of refraction, the more precise the refraction result.

D. Quantization Error

The proposed method uses the effect of refraction. However, that effect should be extremely small. Therefore, this method could be sensitive to error. In this simulation, there is no error in the image coordinates. In practice, however, quantization error will be generated because of the size of the pixel. We usually determine the coordinates to the integer precision of a pixel. In this section, we generate quantization error artificially and inspect the effect of this error to the result of the 3D reconstruction.

During image capture in the simulation, the coordinates of the image points were rounded to zero, one, two and three decimal places. The proposed method was applied to these coordinates. The medium of this simulation was air. The results are shown in Figs. 10 (a)–(d), respectively. It is clear that the coordinates rounded to zero and one decimal places are not precise enough to reconstruct the real positions. We need precision to at least the two decimal place. Therefore, the proposed method requires sub-pixel accuracy for detection of the corresponding points.

V. CONCLUSIONS

In this paper, we proposed a scale-reconstructable Structure from Motion method with a single camera by using refraction and verified its effectiveness in simulation. The
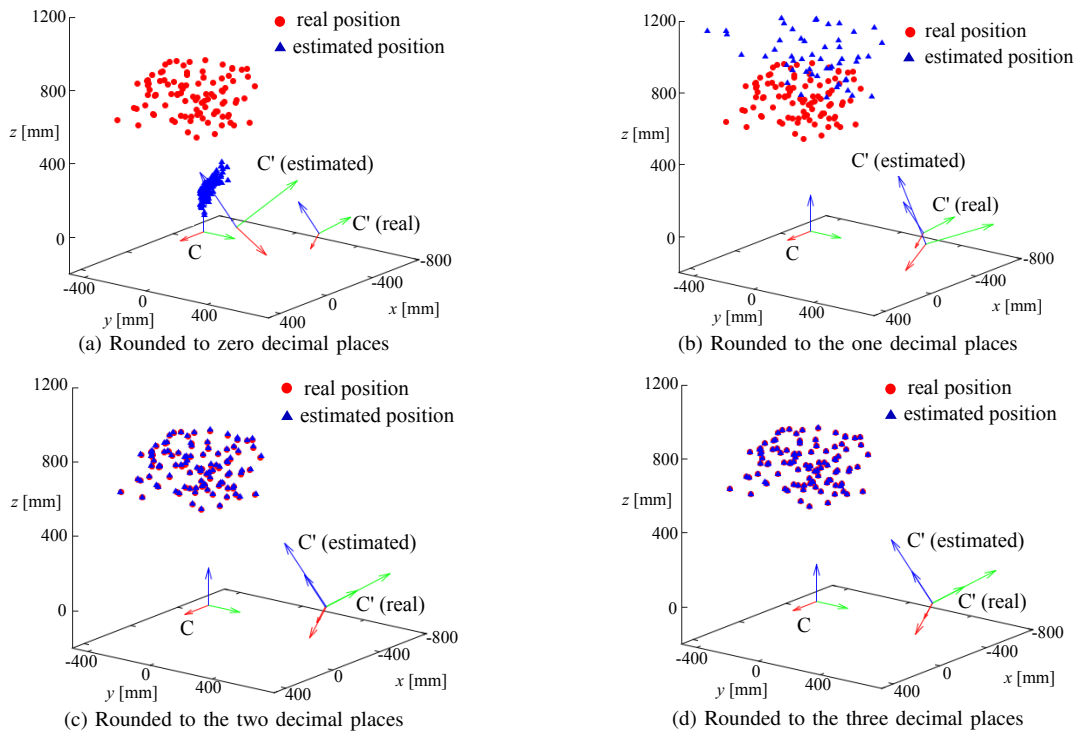
Fig. 10. Results of the proposed method when quantization error exists in the simulation. It is clear that the coordinates rounded to zero and one decimal places are not precise enough to reconstruct the real positions. We need precision to at least the two decimal place.

proposed method is simple because it requires only a refractive plate that causes light rays to change their direction and is attached in front of a single camera. Furthermore, it is clear that this method is applicable to various media such as water as well as air. This indicates that this method could be used for underwater exploration. The experiments also show that the precision of the reconstruction is improved by using a thicker refractive plate because the effect of refraction increases. However, it is also clear that this method is sensitive to error. Even the quantization error has a bad influence on the results of reconstruction. This means that detecting corresponding positions with sub-pixel accuracy is necessary. Therefore, the robustness of this method should be improved.

Experimental results using actual measurements have not been acquired yet. This task will be future work. Furthermore, it would be interesting to examine whether this method would be more accurate when using a special-shaped refractive object instead of a refractive plate.

ACKNOWLEDGMENT

REFERENCES

[1] Richard Hartley and Andrew Zisserman: "Multiple View Geometry in Computer Vision" Cambridge University Press, second edition, 2004.
[2] Davide Scaramuzza, Friedrich Fraundorfer, Marc Pollefeys and Roland Siegwart: "Absolute Scale in Structure from Motion from a Single Vehicle Mounted Camera by Exploiting Nonholonomic Constraints", *Proceedings of the 2009 IEEE International Conference on Computer Vision*, pp.1413–1419, 2009.
[3] Ashwin P. Dani, Nicholas R. Fischer and Warren E. Dixon: "Single Camera Structure and Motion", *IEEE Transactions on Automatic Control*, Vol. 57, No. 1, pp.238–243, 2012.
[4] Manolis Lourakis and Xenophon Zabulis: "Accurate Scale Factor Estimation in 3D Reconstruction", *Proceedings of the International Conference on Computer Analysis of Images and Patterns*, Vol.1, pp.498–506, 2013.
[5] Tali Treibitz, Yoav Y. Schechner and Hanumant Singh: "Flat Refractive Geometry", *Proceedings of the 2008 IEEE Computer Society Conference on Computer Vision and Pattern Recognition*, pp.1–8, 2008.
[6] Visesh Chari and Peter Sturm: "Multi-View Geometry of the Refractive Plane", *Proceedings of British Machine Vision Conference 2009*, pp.1–11, 2009.
[7] Lai Kang, Lingda Wu and Yee-Hong Yang: "Two-View Underwater Structure and Motion for Cameras under Flat Refractive Interfaces", *Proceedings of European Conference on Computer Vision 2011*, pp.303–316, 2012.
[8] Anne Jordt-Sedlazeck and Reinhard Koch: "Refractive Structure-from-Motion on Underwater Images", *Proceedings of the 2013 IEEE International Conference on Computer Vision*, pp.57–64, 2013.
[9] Zhihu Chen, Kwan-Yee K. Wong, Yasuyuki Matsushita, Xiaolong Zhu and Miaomiao Liu: "Self-Calibrating Depth from Refraction", *Proceedings of the 2011 IEEE International Conference on Computer Vision*, pp.635–642, 2011.
[10] Chunyu Gao and Narendra Ahuja: "A Refractive Camera for Acquiring Stereo and Super-resolution Images", *Proceedings of the 2006 IEEE Computer Society Conference on Computer Vision and Pattern Recognition*, pp.2316–2323, 2006.
[11] Doo Hyun Lee, In So Kweon and Roberto Cipolla: "A Biprism-Stereo Camera System", *Proceedings of the 1999 IEEE Computer Society Conference on Computer Vision and Pattern Recognition*, Vol.1, pp.82–87, 1999.
[12] Atsushi Yamashita, Yudai Shirane and Toru Kaneko: "Monocular Underwater Stereo –3D Measurement Using Difference of Appearance Depending on Optical Paths–", *Proceedings of the 2010 IEEE/RSJ International Conference on Intelligent Robots and Systems*, pp.3652–3657, 2010.
[13] Yao-Jen Chang and Tsuhan Chen: "Multi-View 3D Reconstruction for Scenes under the Refractive Plane with Known Vertical Direction", *Proceedings of the 2011 IEEE Computer Society Conference on Computer Vision and Pattern Recognition*, pp.351–358, 2011.